

1 **Direct colorimetry of imipenem decomposition as a novel cost effective method for detecting**  
2 **carabapenamase producing bacteria**

3 **Stathis D. Kotsakis<sup>a\*</sup>, Anastasia Lambropoulou<sup>a</sup>, Georgios Miliotis<sup>a</sup>, Eva Tzelepi<sup>a</sup>, Vivi Miriagou<sup>a</sup>,**  
4 **Leonidas S. Tzouvelekis<sup>a</sup>**

5 <sup>a</sup>Laboratory of Bacteriology, Hellenic Pasteur Institute, Vas. Sofias 127, 115 21 Athens, Greece.

6

7

8

9

10

11

12

13

14

15

16

17

18

19

20

21

22

23

24

25

26

27

28 \*Corresponding author: Dr. Stathis D. Kotsakis, Laboratory of Bacteriology, Hellenic Pasteur Institute.

29 [skotsakis@pasteur.gr](mailto:skotsakis@pasteur.gr)

30

31 **Abstract**

32 In the absence of a molecule that would collectively inhibit both metallo- $\beta$ -lactamases and serine reactive  
33 carbapenemases, containment of their genes' spreading is the main weapon currently available for  
34 confronting carbapenem resistance in hospitals. Cost effective methodologies rapidly detecting  
35 carbapenemase producing enterobacteria (CPE) would facilitate such measures. Herein a low cost CPE  
36 detection method was developed that was based on the direct colorimetry of the yellow shift caused by  
37 the accumulation of diketopiperazines – products of the acid catalyzed imipenem oligomerization –  
38 induced by carbapenemase action on dense solutions of imipenem/cilastatin. The reactions were studied  
39 by spectrophotometry in the visible spectrum using preparations of  $\beta$ -lactamases from the four molecular  
40 classes. The effects of various buffers on reactions containing the potent carbapenemases NDM-1 and  
41 NMC-A were monitored at 405 nm. Optimal conditions were used for the analysis of cell suspensions and  
42 the assay was evaluated using 38 selected enterobacteria including 29 CPE as well as nine carbapenemase-  
43 negative strains overexpressing other  $\beta$ -lactamases. The development of the yellow color was specific for  
44 carbapenemase containing enzyme preparations and the maximum intensity was achieved in acidic or un-  
45 buffered conditions in the presence of zinc. When applied on bacterial cell suspensions the assay could  
46 detect CPE with 96.7 % sensitivity and 100 % specificity with results being comparable to those obtained  
47 with the CARBA NP technique. Direct colorimetry of carbapenemase-induced imipenem decomposition  
48 required minimum reagents while exhibited high accuracy in detecting CPE. Therefore it should be  
49 considered for screening purposes after further clinical evaluation.

50

51

52

53

54 **Importance**

55 Currently, spread of multi-drug resistant (MDR) carbapenemase-producing enterobacteria (CPE), mostly  
56 in the clinical setting, is among the most pressing public health problems worldwide. In order to  
57 effectively control CPE, use of reliable and affordable methods detecting carbapenemase genes or the  
58 respective  $\beta$ -lactamases is of vital importance. Herein we developed a novel method, based on a  
59 previously undescribed phenomenon, which can detect CPE with few reagents by direct colorimetry of  
60 bacterial suspensions and imipenem/cilastatin mixtures.

61

62

63

64

65

66

67

68

69

70

71

72

73

## 74 **Introduction**

75 The development of a single molecule that would collectively inhibit all carbapenemases is a difficult task  
76 due to their different reaction mechanisms (zinc dependent; metallo-beta-lactamases or serine reactive;  
77 classes A and D). Although molecules with such properties are currently being tested (e.g. cyclic  
78 boronates; 1), none has entered the clinical practice and the latest therapeutic  $\beta$ -lactam/ $\beta$ -lactamase  
79 inhibitor combinations encompassing the diazabicyclooctanes class of compounds (e.g. avibactam and  
80 relebactam) are only active against serine reactive enzymes (2). Given that carbapenemase producing  
81 enterobacteria (CPE) are commonly expressing co-resistances to other drugs of choice, the early detection  
82 and confinement of their sources is currently the main way that could confront outbreaks of the respective  
83 infections in a health-care setting (3).

84 A high number of CPE diagnostic techniques are currently available (reviewed in references 4, 5). Yet, only  
85 a handful are suitable for the screening purposes of an infection control approach. An efficient technique  
86 for CPE screening should be high throughput, sensitive and specific, cost effective, able to detect even  
87 unknown carbapenemases while also providing information on the reaction mechanism (M $\beta$ L or serine  
88 reactive). The above criteria are simultaneously satisfied by methodologies which detect the  
89 carbapenemase activity in dense bacterial suspensions using color development (e.g. RAPIDEC CarbaNP,  
90 BlueCarba, beta-CARBA and MAST CARBA PAcE; 6-9). Although the current colorimetric techniques are  
91 relatively low cost, the cumulative financial burden during a screening would be still high for a limited-  
92 budget setting.

93 Recently, during the development of a technique that detects the imipenem acidic hydrolysis product  
94 using an ion sensitive field effect transistor (10) we have observed that reaction mixtures containing CPE  
95 yielded a yellowish color that gradually became more intense - something that did not occur for the  
96 carbapenemase negative strains even after prolonged incubation. This phenomenon most likely resulted

97 from the pH drop during imipenem hydrolysis and was due to the complex oligomerization reactions  
98 taking place in dense solutions of the compound under acidic conditions yielding chromophoric  
99 diketopiperazines (11). Herein we showed that under the experimental conditions of the techniques  
100 detecting carbapenemase production utilizing pH changes, a color shift would occur due to imipenem  
101 decomposition, even in the absence of an indicator and that this can be used as a cost effective alternative  
102 method for CPE screening.

## 103 **Materials and Methods**

### 104 **$\beta$ -Lactamase preparations**

105 Crude protein extracts containing  $\beta$ -lactamases were prepared from laboratory *E. coli* clones replicating  
106 the recombinant plasmids pZE21-*bla*<sub>NDM-1</sub> (*E. coli* C600Z1), pNTN3-*bla*<sub>NMC-A</sub> (*E. coli* JM109), pZE21-*bla*<sub>OXA-48</sub>  
107 (*E. coli* C600Z1), pBC-*bla*<sub>CMY-2</sub> (*E. coli* DH5 $\alpha$ ) and pBC-*bla*<sub>CTX-M-15</sub> (*E. coli* DH5 $\alpha$ ) overexpressing the NDM-1  
108 (M $\beta$ L), NMC-A (class A carbapenemase), OXA-48 (class D carbapenemase), CMY-2 (class C  $\beta$ -lactamase)  
109 and CTX-M-15 (class A  $\beta$ -lactamase -ESBL) enzymes respectively. In pZE21 clones transcription of the  
110 cloned  $\beta$ -lactamase gene was induced by 200 ng/ml anhydrotetracycline while in the remaining plasmids  
111 expression was constitutive driven by natural promoters of the genes. Proteins were released through  
112 sonication (10) in 50 mM sodium phosphate buffer pH 7 with the exception of the M $\beta$ L preparations  
113 where a 50 mM HEPES, 50  $\mu$ M ZnSO<sub>4</sub> pH 7.2 buffer was used. Hydrolysis of imipenem (NDM-1, NMC-A  
114 and OXA-48), cephalothin (CMY-2) or cefotaxime (CTX-M-15) was measured by UV spectrophotometry.  $\beta$ -  
115 Lactamase concentration in the extracts was estimated using the initial velocities and the published steady  
116 state hydrolysis constants (12-16) by the *Michaelis-Menten* equation.

### 117 **Bacterial strains and susceptibility testing**

118 A total of 38 non-repetitive enterobacterial strains were used in the study. These included 29 strains  
119 producing a carbapenemase and nine strains producing  $\beta$ -lactamases with either marginal or no

120 carbapenem hydrolytic activity (non-carbapenemases). The detailed  $\beta$ -lactamase content of each strain is  
121 given in Table 1. Isolates had been previously characterized using phenotypic and molecular techniques  
122 (17, 18). The uniqueness of strains belonging in the same species and exhibiting identical  $\beta$ -lactamase  
123 content was asserted through restriction fragment length polymorphism analysis using pulsed field gel  
124 electrophoresis. All strains had been isolated from clinical settings in Greece, save for the IMP producers  
125 that were of environmental origin (19).

126 Imipenem and meropenem MICs were determined using the microdilution method in Mueller-Hinton  
127 broth according to the EUCAST recommendations. Carbapenems were tested at a concentration range  
128 from 0.125 to 128  $\mu\text{g/ml}$ .

#### 129 **Spectrophotometric analyses of imipenem decomposition in the visible**

130 In spectrophotometric analyses a stock solution of 10 mg/ml imipenem – 10 mg/ml cilastatin was used. It  
131 was prepared from a generic 500+500 mg imipenem/cilastatin powder for injection containing also 1.6  
132 mmol of sodium bicarbonate ( $\text{NaHCO}_3$ ). Reconstitution was carried out using either a solution of 0.3 mM  
133 zinc sulfate ( $\text{ZnSO}_4$ ) or de-ionized water and the resulting suspensions were aliquoted and stored at -80  
134  $^\circ\text{C}$  until further use.

135 Acquisition of absorbance spectra was carried out using a HITACH U-2001 UV/Vis double beam  
136 spectrophotometer in a quartz cuvette of 1 cm optical path. Each reaction had a volume of 1 ml and was  
137 prepared through 1:1 dilution of the imipenem/cilastatin- $\text{ZnSO}_4$  stock solution in deionized water that  
138 resulted in the following composition: 5 mg/ml imipenem, 5 mg/ml cilastatin, 16 mM  $\text{NaHCO}_3$  and 0.15  
139 mM  $\text{ZnSO}_4$  with the pH being  $7.2\pm 0.1$ . Quantities of the  $\beta$ -lactamase preparations were added in the  
140 reaction mixture - with the buffering salt included in the crude protein extract having a final concentration  
141 of no more than 2 mM - and the spectrum from 342 nm to 1100 nm was scanned at a rate of 800 nm $\cdot$ min $^{-1}$   
142 <sup>1</sup> at various time intervals. Differential absorption spectra were obtained through subtraction of the initial

143 spectrum from the spectra obtained at each time point. A control reaction lacking a  $\beta$ -lactamase was also  
144 performed as above.

145 The effects of zinc, pH and various buffers on the carbapenemase induced color development were  
146 examined using a DYNEX MRX absorbance micro-plate reader. Readings were obtained at 405 nm with  
147 the reference filter being set at 630 nm. Here the imipenem/cilastatin-water stock solution was used that  
148 was diluted 1:1 either in i) deionized water, ii) 0.1 M 2-(N-morpholino)-ethanesulfonic acid (MES) pH 5.4,  
149 iii) 0.1 M 3-(N-morpholino)-propanesulfonic acid (MOPS) pH 6.9, iv) 0.1 M MOPS pH 7.2 or v) 0.1 M  
150 Tris/HCl pH 8. The same solutions supplemented with 0.3 mM ZnSO<sub>4</sub> were also assayed. Reactions were  
151 prepared directly on the microplate's wells and had a volume of 100  $\mu$ l. The NDM-1 M $\beta$ L and the NMC-A  
152 class A carbapenemases were tested and results were compared with those of control wells.

153 The effects of NDM-1 and NMC-A carbapenemases on 5 mg/ml of imipenem (imipenem hydrate  $\geq$ 98%,  
154 Cayman Chemicals) solution containing 16 mM NaHCO<sub>3</sub> and 0.15 mM ZnSO<sub>4</sub> as well as on 5 mg/ml  
155 imipenem – 5 mg/ml cilastatin in 0.15 mM ZnSO<sub>4</sub> prepared from the brand name Primaxin formulation  
156 (Merck, Sharp & Dohme Corp.) were also examined.

#### 157 **Analysis of bacterial suspensions with the imipenem decomposition method**

158 Dense cell suspensions were prepared by the addition of two full 10  $\mu$ L plastic inoculation loops (Sarstedt,  
159 Germany) of bacteria grown on Tryptone Soya Agar (TSA; OXOID-Thermo Scientific, UK), supplemented  
160 with 0.3 mM ZnSO<sub>4</sub>, into 400  $\mu$ L of H<sub>2</sub>O. For each strain, 50  $\mu$ L of this suspension were added into four  
161 wells of a 96-well micro-plate (polystyrene flat bottom clear wells; Greiner, Germany). Fifty microliters of  
162 the imipenem/cilastatin-ZnSO<sub>4</sub> stock solution were added in two of the above wells while in the remaining  
163 two, introduced for absorbance correction, the same volume of a 0.3 mM ZnSO<sub>4</sub> solution was added  
164 (control 1). Wells containing the Imipenem/cilastatin- ZnSO<sub>4</sub> (control 2) and ZnSO<sub>4</sub> solutions (control 3)  
165 diluted 1:1 with H<sub>2</sub>O were also included as controls. The plates were incubated at 37 °C and the

166 absorbance was measured using a DYNEX MRX micro-plate reader at various time points. The absorbance  
167 of the wells containing the mixtures of bacterial suspensions with imipenem/cilastatin were corrected by  
168 subtracting that of control 1 and control 2 (control 3 corrected) wells. Each experiment was performed in  
169 triplicate. Estimation of a threshold of absorbance increase in order to characterize a strain as a  
170 carbapenemase producer was carried out through Receiver Operating Characteristic (ROC) analysis with  
171 Prism v. 8.0. Absorbance changes documented in experiments of carbapenemase negative strains were  
172 grouped in the “Control column” and those of positive strains in the “Patients” column. An absorbance  
173 increase greater than 0.0456 yielded 96.55% sensitivity (95% Confidence Interval, CI: 82.82 – 99.82%) and  
174 100% specificity (95% CI: 97.23 – 100.00%). Hence the threshold was set at 0.05 of absorbance increase.

175 The effect of metal chelation on color development was assessed by the addition of EDTA (0.5 M pH 8) in  
176 the bottom of the wells before the various reaction components and by preparing the bacterial  
177 suspensions in EDTA containing solutions. The concentrations of EDTA included in the reaction during  
178 preliminary experiments were 10 and 15 mM with the former being selected as optimum. In these  
179 experiments bacteria grown on TSA without zinc supplementation were also tested.

#### 180 **Comparisons with the CARBA NP technique**

181 Direct colorimetry was compared with the commercial pH indicator colorimetric technique RAPIDEC  
182 CARBANP (bioMerieux, France). For these comparisons we included strains expected to cause sensitivity  
183 and specificity issues in CPE detection techniques. Bacteria were grown on TSA containing 0.3 mM ZnSO<sub>4</sub>  
184 at 37 °C for 16 h and the assay was performed and interpreted according to the manufacturer’s  
185 instructions.

186

187

188



## 189 **Results and discussion**

### 190 **Spectrophotometric analyses of $\beta$ -lactamase – imipenem/cilastatin mixtures in the visible**

191  $\beta$ -Lactam hydrolysis is accompanied by shifts in absorption in the UV spectrum due to the opening of the  
192 four member ring. The fact that carbapenemase action on imipenem solutions in the absence of a pH  
193 buffer leads to absorbance changes in the visible region of the light spectrum, as the yellow color  
194 development indicated, prompted us to study the phenomenon through spectrophotometry.

195 The differential absorption spectra (Figure 1A) in carbapenemase containing reactions showed the  
196 accumulation of species that absorb in the violet region. The efficient carbapenemases NDM-1 and NMC-  
197 A assayed at nanomolar quantities induced shifts which were apparent after 15 minutes. The less potent  
198 OXA-48 required longer reaction times and sub-micromolar quantities in order to observe the absorbance  
199 increases in the violet region (Figure 1A, upper panel). On the other hand, CMY-2 and CTX-M-15 – enzymes  
200 that do not exhibit meaningful imipenemase activity – yielded only minor absorbance increases after  
201 three hours, similarly with what was observed in the control reaction containing solely  
202 imipenem/cilastatin (Figure 1A, lower panel). Therefore, the color shift was a phenomenon that was  
203 specifically observed for carbapenemases.

204 Multiple peaks were apparent with the  $\lambda_{\max}$  initially being 360 nm and then increased with time up to 370  
205 nm. In the highly efficient NDM-1 and NMC-A, after three hours of incubation a second peak became  
206 predominant in the area of 400 nm while absorbance in the previous peak remained stable (Figure 1A).  
207 The above data indicated that the reactions taking place during the action of carbapenemases resulted in  
208 the formation of more than one chromogenic products. By plotting the absorbance in various wavelengths  
209 it was apparent that the carbapenemase activity could also be detected at 405 nm, though requiring  
210 longer reaction times (Figure 1B). Hence, the carbapenemase induced color shift could be quantified in a

211 Clinical Microbiology laboratory through the widely available micro-plate absorbance readers instead of  
212 a UV/Vis spectrophotometer used here.

### 213 **Effects of various solutions on carbapenemase induced color formation**

214 The effects of different buffers at various pH values in the presence and absence of zinc(II) on the  
215 occurrence of the yellowish color were assessed. In NDM-1 containing reactions the color development  
216 was dependent on zinc, especially at the acidic pH of the MES buffer as well as in un-buffered conditions,  
217 contrary to NMC-A and control experiments (Figure 2A). Coloration induced by NMC-A was dependent on  
218 the pH and the buffering capacity of the solution. The highest absorbance increases were observed in  
219 reactions which did not contain a buffering salt (i.e. H<sub>2</sub>O or 15 mM ZnSO<sub>4</sub> reactions) and in the MES buffer  
220 at pH 5.4 (Figure 2A; right graph column). In the presence of MOPS, phosphate and Tris buffers the color  
221 development was significantly attenuated as the alkalinity of the reaction environment increased (Figures  
222 2A and 2B). Similar observations were made for NDM-1 in zinc supplemented solutions (Figures 2A and  
223 2B). In control reactions containing only imipenem a moderate absorbance increase was observed in the  
224 acidic MES buffer irrespective of zinc ions with the remaining solutions being inert (Figure 2A; left graph  
225 column). The specific requirement for Zn(II) in MβL reactions provided additional evidence that the  
226 phenomenon is indeed induced by the enzymatic hydrolysis of imipenem. It has been shown that low pH  
227 has a detrimental effect on MβL activity - probably due to the protonation of Asp120 of the second Zn(II)  
228 binding site that results in loss of one of the zinc ions – and that this can be countered by zinc  
229 supplementation of the reaction buffer (20, 21).

230 The dependence of the carbapenemase induced color development on acidic pH or the absence of a  
231 buffering agent provided some evidence on the likely molecular bases of the phenomenon. It is known  
232 from stability studies of imipenem and the imipenem/cilastatin formulation that the compound  
233 decomposes in acidic pH at concentrations  $\geq 1$  mg/ml through complex oligomerization reactions that lead

234 to the formation of diketopiperazines yielding yellow colored solutions (11, 22-25). Hence, a possible  
235 explanation for our data would be that as the enzymes hydrolyze the  $\beta$ -lactam ring of imipenem and the  
236 acidic hydrolysis product is accumulated, the pH is decreased triggering thus secondary decomposition  
237 reactions leading to the formation of chromogenic diketopiperazines (Figure 2C - compounds VI and VIII;  
238 11).

239 The developed assay requires increased quantities of the substrate and hence, to decrease the cost, we  
240 have used a commercially available generic imipenem/cilastatin formulation. In order to assert that the  
241 observed phenomenon is governed by the above mechanism we assayed pure imipenem and the brand-  
242 name imipenem/cilastatin formulation (Primaxin). After 60 minutes of incubation the yellow color was  
243 developed in all reactions, with those of imipenem/cilastatin yielding stronger signals (Figure 2D). At 2  
244 hours though, the color in the imipenem solution started to fade, indicating consumption of the  
245 chromophore product, in contrast to the imipenem/cilastatin solutions (Figure 2D). The above results  
246 suggested that imipenem oligomerization caused by the acidification induced by the action of  
247 carbapenemases may indeed be the reason for the color development, at least in the initial reactions,  
248 with cilastatin having a yet unknown key role.

#### 249 **Development of a CPE screening tool**

250 As assays with enzyme preparations indicated that the color development due to imipenem  
251 decomposition was specific for carbapenemases we subsequently explored the use of this method as a  
252 diagnostic tool by testing cell suspensions of clinical isolates. Although the color shift was visually  
253 detectable we quantified it through absorbance measurements at 405 nm using a micro-plate reader to  
254 improve objectivity.

255 The majority of the M $\beta$ L producing enterobacteria exhibited rapid color shifts that were also reflected on  
256 the measured absorbance (Figure 3; Table 1). The weakest responses were observed with VIM-1

257 expressing strains with three of them requiring more than 60 minutes incubation in order the yellow color  
258 to develop (Figure 3). Nonetheless, all 15 M $\beta$ L producers yielded high intensity end-point coloration with  
259 the maximum absorbance at 405 nm being in the range of 0.39 to 0.43 units (Figure 3; Table 1). Fast color  
260 development was also evident for all KPC-2 class A carbapenemase producers tested with the maximum  
261 absorbance values ranging from 0.49 to 0.71 (Figure 3; Table 1). Production of the less efficient OXA-48  
262 class D carbapenemase required longer incubation times in order to be detected through the imipenem  
263 decomposition method with the yellow color developing after 90 to 120 minutes (Figure 3). Furthermore  
264 two strains, isolated in the initial stages of the OXA-48 epidemic in the Near East, yielded marginal or no  
265 color shifts (*K. pneumoniae* TRK-5 and TRK-1; Figure 3). These strains were found negative with CARBA NP  
266 (Table 2). In the six OXA-48 producing strains that yielded a response the maximum absorbance varied  
267 between 0.06 and 0.57. The nine isolates not producing a carbapenemase but overexpressing other  $\beta$ -  
268 lactamases did not yield any coloration even after six hours of incubation (Figure 3). The maximum  
269 absorbance values observed for these strains ranged between -0.002 to 0.01 units (Table 1). By applying  
270 the threshold estimated trough ROC analysis the method could detect 16 out of 16 of the M $\beta$ L strains  
271 within <30-180 minutes, 5/5 of KPC-2 producers in less than 30 minutes, and 6/7 of OXA-48 isolates in 90  
272 to 360 minutes while it excluded all the non carbapenemase producers as negatives (Table 1). Of note,  
273 two of the carbapenemase negative isolates (*K. pneumoniae* EY-205 and 17829) gave false positive results  
274 when analyzed with the CARBA NP technique (Table 2). The obtained data indicated that direct  
275 colorimetry could detect CPE with 96.4% sensitivity (1/28 false negatives) and 100% specificity (0/9 false  
276 positives).

277 The ability of this method to discriminate between M $\beta$ L and serine reactive carbapenemase producers  
278 was assessed using EDTA as a chelating agent. Preliminary experiments were performed using 10 and 15  
279 mM EDTA in the reaction mixtures. At these concentrations the color formation observed in M $\beta$ L  
280 producing strains was attenuated but a quenching in the coloration induced by KPC-2 producers was

281 observed, probably due to an increase of the solution's alkalinity (Supplemental Figure 1). Hence, 10 mM  
282 was selected as an optimal EDTA concentration. EDTA could efficiently inhibit the yellow color induced by  
283 suspensions of NDM producing bacteria as well as of some VIM and IMP producing strains with  
284 insignificant effects on signals obtained from serine reactive carbapenemase producers (Figure 4). Color  
285 formation in the presence of EDTA was evident with a VIM-1 producing *K. pneumoniae* (Kpn LA30) and a  
286 *P. mirabilis* strain expressing the IMP-4 enzyme (Figure 4A, right panel). Considering that the yellow color  
287 is formed indirectly through secondary reactions and not due to the direct action of carbapenemases,  
288 then any residual imipenem hydrolysis may initiate the cascade leading to a positive result. In order to  
289 overcome this we performed the same experiments with the bacterial suspensions being prepared in  
290 EDTA which was then mixed with the imipenem/cilastatin solution. This modification permitted the  
291 inhibition of *K. pneumoniae* LA30 reactions but not those of the *P. mirabilis* IMP-4 strain that was still able  
292 to yield a strong coloration (Figure 4A and C). The above may be due to the relative resistance of IMP  
293 enzymes to the action of EDTA combined with increased levels of the enzyme in the bacterium's  
294 periplasm.

295 Indeed, as the strains were grown on zinc supplemented media, in order to assert high periplasmic levels  
296 of fully functional MβLs, the observed resistance of the color formation to EDTA inhibition may be due to  
297 increased enzyme quantities released in the solution. In order to assess this we performed the same set  
298 of experiments with strains grown on plain TSA. The results showed that without zinc supplementation,  
299 the color development could be inhibited by EDTA in the majority of the MβL producing strains (Figure  
300 4A, left panel). However *P. mirabilis* EUG91, that produces low quantities of VIM-1 (10), failed to give a  
301 positive reaction even after six hours of incubation. Thus, EDTA inhibition could be used for the  
302 identification of MβL producers with the above method when bacteria are cultured without excess zinc  
303 but this would reduce the sensitivity for some strains exhibiting low levels of functional periplasmic MβLs.

304 The color development induced by suspensions of serine reactive carbapenemase producing  
305 enterobacteria remained relatively unaffected by EDTA (Figure 4B and C). It should be noted that in OXA-  
306 48 producers the chelator increased the color intensity, probably through the release of more enzyme in  
307 the solution facilitated by its detrimental effect on cell wall integrity (Figure 4B). Zinc supplementation of  
308 the growth media seemed to affect the chromogenic reaction of positive strains yielding systematically  
309 lower end point absorbance increases even for the M $\beta$ L producing isolates ( $\Delta OD^{TSA-max, TSA+ZnSO4-max} =$   
310  $0.26 \pm 0.12$ , paired t-test  $p < 0.001$ ). Zinc ions are known to have a variety of effects on bacterial physiology  
311 (26) and therefore we cannot yet provide an explanation for the above observation. Strains not producing  
312 a carbapenemase remained negative under all the employed modifications of the method.

313 Based on these data the use of direct colorimetry combined with various chelating agents in order to  
314 distinguish M $\beta$ L from serine carbapenemase producers warrants further study.

## 315 **Conclusions**

316 Imipenem is the first clinically used carbapenem that exhibits increased stability to aminolysis compared  
317 to its natural counterpart thienamycin. Yet, the molecule still possesses an inherent instability in aqueous  
318 solutions as compared to newer carbapenems (e.g. meropenem; 27, 28). Indeed its decomposition in low  
319 pH results in complex degradation products not observed in the other members of the group (29). Herein  
320 we showed that the accumulation of chromophoric decomposition products of imipenem in the acidic  
321 conditions induced by the action of carbapenemases can be used for the specific detection of CPE directly  
322 from bacterial suspensions.

323 Direct colorimetry required minimum reagents i.e. a solution of 10 mg/ml imipenem-10 mg/ml cilastatin  
324 containing 0.3 mM zinc sulfate and can be prepared from any imipenem/cilastatin powder formulation  
325 for injection used in hospitals. The development of yellow color can be followed either through manual  
326 inspection or with a microplate reader capable of measuring absorbance at 405 nm that would increase

327 both through-put and objectivity. The cost of the method would be significantly lower (>100 fold)  
328 compared to the current commercial CPE detection colorimetric techniques, considering that a 500 mg  
329 imipenem/500 mg cilastatin vial (valued at 6.00 €, Greek market consumer prices; 30) would be sufficient  
330 for 500 reactions. Moreover, as direct colorimetry exhibited high accuracy in detecting CPE and  
331 discriminating non-carbapenemase producers, it fulfills the requirements of a successful CPE screening  
332 technique and merits further evaluation in a variety of clinical settings.

### 333 **Acknowledgements**

334 We thank Dr. Angeliki Mavroidi, Department of Microbiology, Konstantopouleio-Patission General  
335 Hospital of Athens Greece, for providing *K. pneumoniae* OXA-48 producing strains as well as Dr. Monika  
336 Dolejska and Dr. Iva Kutilova, Department of Biology and Wildlife Diseases, University of Veterinary and  
337 Pharmaceutical Sciences Brno Czech Republic, for providing the IMP producing enterobacterial strains.

### 338 **References**

- 339 1. Cahill ST, Cain R, Wang DY, Lohans CT, Wareham DW, Oswin HP, Mohammed J, Spencer J, Fishwick  
340 CW, McDonough MA, Schofield CJ, Brem J. 2017. Cyclic boronates inhibit all classes of beta-  
341 lactamases. *Antimicrob Agents Chemother* 61.
- 342 2. Bush K, Bradford PA. 2019. Interplay between beta-lactamases and new beta-lactamase  
343 inhibitors. *Nat Rev Microbiol* 17:295-306.
- 344 3. Tzouvelekis LS, Markogiannakis A, Psychogiou M, Tassios PT, Daikos GL. 2012. Carbapenemases in  
345 *Klebsiella pneumoniae* and other Enterobacteriaceae: an evolving crisis of global dimensions. *Clin*  
346 *Microbiol Rev* 25:682-707.
- 347 4. Aguirre-Quinonero A, Martinez-Martinez L. 2017. Non-molecular detection of carbapenemases in  
348 Enterobacteriaceae clinical isolates. *J Infect Chemother* 23:1-11.
- 349 5. Bilozor A, Balode A, Chakhunashvili G, Chumachenko T, Egorova S, Ivanova M, Kaftyreva L, Koljalg  
350 S, Koressaar T, Lysenko O, Miciuleviciene J, Mandar R, Lis DO, Wesolowska MP, Ratnik K, Remm  
351 M, Rudzko J, Roop T, Saule M, Sepp E, Shyshporonok J, Titov L, Tsereteli D, Naaber P. 2019.  
352 Application of molecular methods for carbapenemase detection. *Front Microbiol* 10:1755.
- 353 6. Nordmann P, Poirel L, Dortet L. 2012. Rapid detection of carbapenemase-producing  
354 Enterobacteriaceae. *Emerg Infect Dis* 18:1503-7.
- 355 7. Pires J, Novais A, Peixe L. 2013. Blue-carba, an easy biochemical test for detection of diverse  
356 carbapenemase producers directly from bacterial cultures. *J Clin Microbiol* 51:4281-3.

- 357 8. Bernabeu S, Dortet L, Naas T. 2017. Evaluation of the beta-CARBA test, a colorimetric test for the  
358 rapid detection of carbapenemase activity in Gram-negative bacilli. *J Antimicrob Chemother*  
359 72:1646-1658.
- 360 9. Rezzoug I, Emeraud C, Sauvadet A, Cotellon G, Naas T, Dortet L. 2021. Evaluation of a colorimetric  
361 test for the rapid detection of carbapenemase activity in Gram negative bacilli: the MAST(R) PACE  
362 test. *Antimicrob Agents Chemother* doi:10.1128/AAC.02351-20.
- 363 10. Kotsakis SD, Miliotis G, Tzelepi E, Tzouvelekis LS, Miriagou V. 2021. Detection of carbapenemase  
364 producing enterobacteria using an ion sensitive field effect transistor sensor. *Sci Rep* 11:12061.
- 365 11. Ratcliffe RW, Wildonger KJ, Di Michele L, Douglas AW, Hajdu R, Goegelman RT, Springer JP,  
366 Hirshfield J. 1989. Studies on the structures of imipenem, dehydropeptidase I-hydrolyzed  
367 imipenem, and related analogs. *The Journal of Organic Chemistry* 54:653-660.
- 368 12. Docquier JD, Calderone V, De Luca F, Benvenuti M, Giuliani F, Bellucci L, Tafi A, Nordmann P, Botta  
369 M, Rossolini GM, Mangani S. 2009. Crystal structure of the OXA-48 beta-lactamase reveals  
370 mechanistic diversity among class D carbapenemases. *Chem Biol* 16:540-7.
- 371 13. Hachler H, Kotsakis SD, Tzouvelekis LS, Geser N, Lehner A, Miriagou V, Stephan R. 2013.  
372 Characterisation of CTX-M-117, a Pro174Gln variant of CTX-M-15 extended-spectrum beta-  
373 lactamase, from a bovine *Escherichia coli* isolate. *Int J Antimicrob Agents* 41:94-5.
- 374 14. Kotsakis SD, Papagiannitsis CC, Tzelepi E, Tzouvelekis LS, Miriagou V. 2009. Extended-spectrum  
375 properties of CMY-30, a Val211Gly mutant of CMY-2 cephalosporinase. *Antimicrob Agents*  
376 *Chemother* 53:3520-3.
- 377 15. Marcoccia F, Bottoni C, Sabatini A, Colapietro M, Mercuri PS, Galleni M, Kerff F, Matagne A,  
378 Celenza G, Amicosante G, Perilli M. 2016. Kinetic Study of Laboratory Mutants of NDM-1 Metallo-  
379 beta-Lactamase and the Importance of an Isoleucine at Position 35. *Antimicrob Agents*  
380 *Chemother* 60:2366-72.
- 381 16. Mariotte-Boyer S, Nicolas-Chanoine MH, Labia R. 1996. A kinetic study of NMC-A beta-lactamase,  
382 an Ambler class A carbapenemase also hydrolyzing cephamycins. *FEMS Microbiol Lett* 143:29-33.
- 383 17. Kotsakis SD, Petinaki E, Scopes E, Siatravani E, Miriagou V, Tzelepi E. 2013. Laboratory evaluation  
384 of Brilliance CRE Agar for screening carbapenem-resistant Enterobacteriaceae: Performance on a  
385 collection of characterised clinical isolates from Greece. *J Glob Antimicrob Resist* 1:85-90.
- 386 18. Voulgari E, Miliotis G, Siatravani E, Tzouvelekis LS, Tzelepi E, Miriagou V. 2020. Evaluation of the  
387 performance of Acuitas(R) Resistome Test and the Acuitas Lighthouse(R) software for the  
388 detection of beta-lactamase-producing microorganisms. *J Glob Antimicrob Resist* 22:184-189.
- 389 19. Dolejska M, Masarikova M, Dobiasova H, Jamborova I, Karpiskova R, Havlicek M, Carlile N, Priddel  
390 D, Cizek A, Literak I. 2016. High prevalence of *Salmonella* and IMP-4-producing  
391 Enterobacteriaceae in the silver gull on Five Islands, Australia. *J Antimicrob Chemother* 71:63-70.
- 392 20. Davies AM, Rasia RM, Vila AJ, Sutton BJ, Fabiane SM. 2005. Effect of pH on the active site of an  
393 Arg121Cys mutant of the metallo-beta-lactamase from *Bacillus cereus*: implications for the  
394 enzyme mechanism. *Biochemistry* 44:4841-9.
- 395 21. Rasia RM, Vila AJ. 2002. Exploring the role and the binding affinity of a second zinc equivalent in  
396 *B. cereus* metallo-beta-lactamase. *Biochemistry* 41:1853-60.
- 397 22. Smith GB, Dezeny GC, Douglas AW. 1990. Stability and kinetics of degradation of imipenem in  
398 aqueous solution. *J Pharm Sci* 79:732-40.
- 399 23. Smith GB, Schoenewaldt EF. 1981. Stability of N-formimidoylthienamycin in aqueous solution. *J*  
400 *Pharm Sci* 70:272-6.



- 401 24. Testa B, Mayer JM. 2003. Hydrolysis in drug and prodrug metabolism: chemistry, biochemistry,  
402 and enzymology. Wiley-VCH, Zürich ; Weinheim.
- 403 25. Zaccardelli DS, Krcmarik CS, Wolk R, Khalidi N. 1990. Stability of imipenem and cilastatin sodium  
404 in total parenteral nutrient solution. JPEN J Parenter Enteral Nutr 14:306-9.
- 405 26. Blencowe DK, Morby AP. 2003. Zn(II) metabolism in prokaryotes. FEMS Microbiol Rev 27:291-311.
- 406 27. Takasu Y, Yoshida M, Tange M, Asahara K, Uchida T. 2015. Prediction of the stability of  
407 meropenem in intravenous mixtures. Chem Pharm Bull (Tokyo) 63:248-54.
- 408 28. Testa B, Mayer JM. 2003. Hydrolysis in drug and prodrug metabolism : chemistry, biochemistry,  
409 and enzymology. Wiley-VCH, Zürich ; Weinheim.
- 410 29. Takeuchi Y, Sunagawa M, Isobe Y, Hamazume Y, Noguchi T. 1995. Stability of a 1 beta-  
411 methylcarbapenem antibiotic, meropenem (SM-7338) in aqueous solution. Chem Pharm Bull  
412 (Tokyo) 43:689-92.
- 413 30. Galinos. 2022. Greek Pharmaceuticals Guide, Imipenem+Cilastatin.  
414 <https://www.galinos.gr/web/drugs/main/drugs/imipenem-cilastatin>. Accessed 12 March.
- 415

416  
417  
418

419

420  
421  
422  
423  
424  
425  
426  
427  
428  
429  
430  
431  
432  
433  
434  
435  
436  
437  
438  
439  
440  
441  
442

443 **Tables**

444 **Table 1:** Clinical strains used in the study and absorbance changes at 405 nm during incubation of  
 445 bacterial suspensions with 5 mg/ml imipenem/cilastatin.

446 Strain	β-lactamases	Max ΔA <sub>405 nm</sub>	t <sub>ΔA&gt;0.05</sub> (min)	MIC (μg/ml)	
				447 Imipenem	Meropenem
448 <b>VIM MβL producers</b>					
449 <i>K. pneumoniae</i> IK14	VIM-1, CMY-2 type	0.53±0.01	90	1	0.5
450 <i>K. pneumoniae</i> LA30	VIM-1, CMY-2 type	0.57±0.01	<30	8	16
451 <i>E. coli</i> TZ116	VIM-1, CMY-13	0.54±0.01	<30	4	1
452 <i>E. cloacae</i> SEC6	VIM-1	0.53±0.05	120-180	1	1
453 <i>P. mirabilis</i> EUG91	VIM-1, VEB-1	0.39±0.01	120	4	≤0.125
454 <b>NDM MβL producers</b>					
455 <i>K. pneumoniae</i> LA26	NDM-1, CTX-M-15	0.42±0.07	<30	16	32
456 <i>K. pneumoniae</i> LA27	NDM-1, CTX-M-15	0.48±0.05	<30	8	8
457 <i>K. pneumoniae</i> LA28	NDM-1, CTX-M-15	0.63±0.01	<30	8	64
458 <i>K. pneumoniae</i> 2489	NDM-1, CTX-M-15	0.41±0.02	<30	32	64
459 <i>K. pneumoniae</i> LA	NDM-1, CTX-M-15	0.59±0.05	<30	8	64
460 <i>K. aerogenes</i> 7362	NDM-1	0.61±0.07	<30		
461 <b>IMP MβL producers</b>					
462 <i>K. pneumoniae</i> 1733	IMP-4	0.53±0.06	<30	ND	1
463 <i>E. coli</i> 1543m1	IMP-4	0.49±0.05	<30	ND	4
464 <i>E. coli</i> 1586m1	IMP-38	0.45±0.05	<30	ND	0.5
465 <i>E. cloacae</i> 1537m	IMP-4	0.47±0.03	<30	ND	8
466 <i>P. mirabilis</i> 1539p	IMP-4	0.39±0.03	<30	ND	8
467 <b>KPC-2 class A carbapenemase producers</b>					
468 <i>K. pneumoniae</i> E971	KPC-2, SHV-5 type	0.49±0.05	60	1	8
469 <i>K. pneumoniae</i> E1370	KPC-2	0.62±0.01	<30	2	4
470 <i>K. pneumoniae</i> E1505	KPC-2	0.68±0.04	<30	32	16
471 <i>E. coli</i> LAR373	KPC-2	0.71±0.03	<30	2	1
472 <i>E. coli</i> LAR152	KPC-2, CTX-M, OXA-1	0.49±0.07	<30	2	2
473 <b>OXA-48 class D carbapenemase producers</b>					
474 <i>K. pneumoniae</i> ALX47	OXA-48, CTX-M-15	0.23±0.02	180	4	8
475 <i>K. pneumoniae</i> LAR478	OXA-48, CTX-M-15	0.13±0.01	240	8	8
476 <i>K. pneumoniae</i> AO2085	OXA-48, CTX-M-15	0.31±0.03	180	ND	ND
477 <i>K. pneumoniae</i> AO1938	OXA-48, CTX-M-15	0.32±0.03	180	ND	ND
478 <i>K. pneumoniae</i> NQ3083	OXA-48	0.57±0.05	90	8	4
479 <i>K. pneumoniae</i> NQ4129	OXA-48	0.47±0.03	90	4	4
480 <i>K. pneumoniae</i> TRK1	OXA-48, CTX-M-15	-0.04±0.04	NA	8	32
481 <i>K. pneumoniae</i> TRK5	OXA-48, CTX-M-15	0.06±0.04	360	16	32
482 <b>Carbapenemase negative strains</b>					
483 <i>K. pneumoniae</i> TZ59	species specific SHV	-0.002±0.003	NA	≤0.125	≤0.125
484 <i>K. pneumoniae</i> IPT59	GES-7, SHV-5	0.01±0.03	NA	0.25	≤0.125
485 <i>K. pneumoniae</i> 17829	CTX-M-15, SHV-12	-0.01±0.01	NA	16	16
486 <i>K. pneumoniae</i> EY-205	CMY-36, SHV-5	0.002±0.03	NA	0.25	≤0.125
487 <i>K. aerogenes</i> EY-25	LAT-2+SHV-5	-0.01±0.03	NA	16	8
488 <i>E. cloacae</i> WTEY-138	derepressed AmpC	0.009±0.1	NA	0.5	≤0.125
489 <i>E. coli</i> IK33	CTX-M-15	0.003±0.006	NA	≤0.125	≤0.125
490 <i>E. coli</i> S13	CTX-M-32	0.009±0.005	NA	≤0.125	≤0.125
491 <i>K. aerogenes</i> EY15	LAT-2	0.007±0.004	NA	8	4

492 ND: Not determined, NA: Not applicable

493

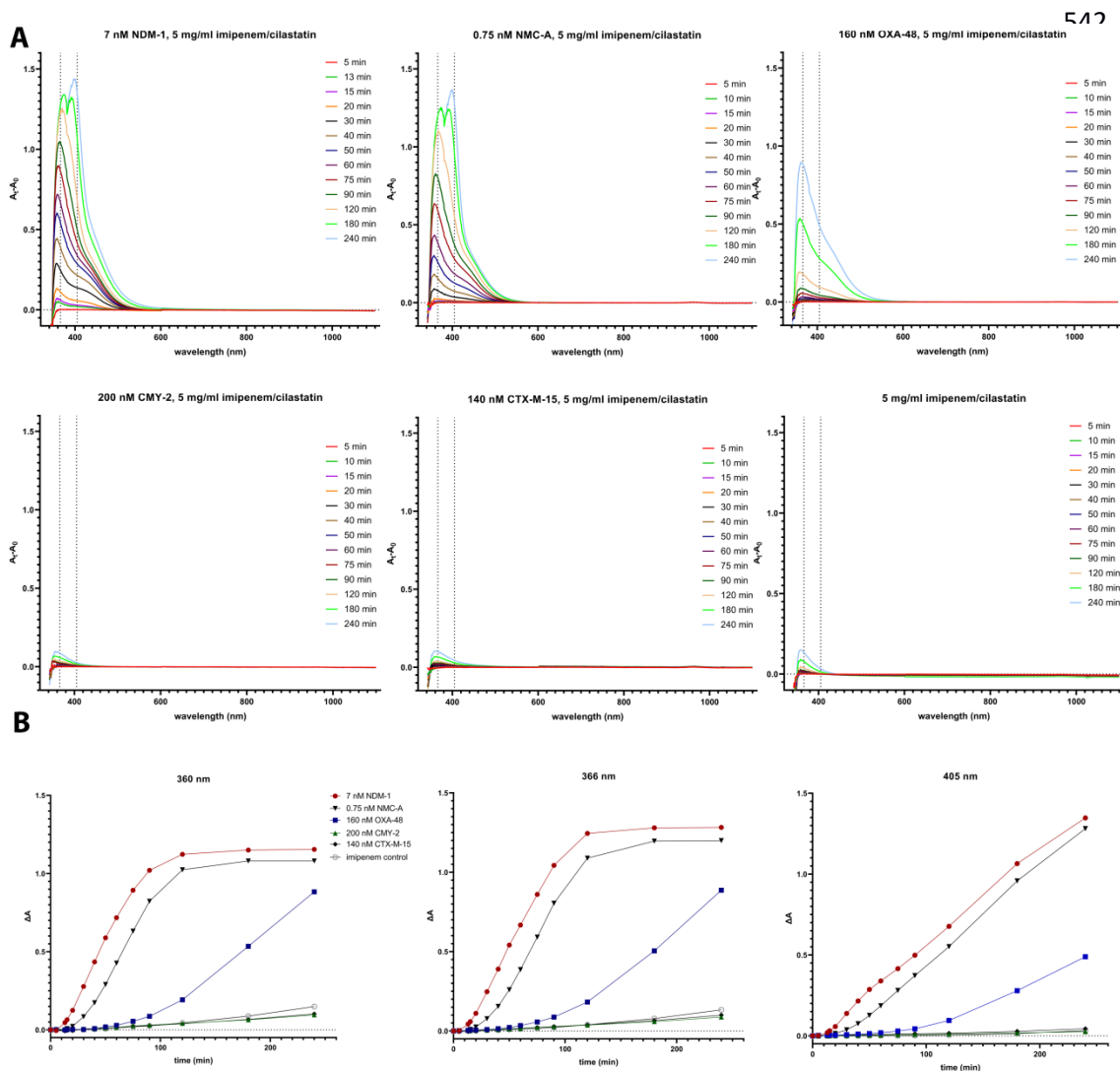
494

495 **Table 2:** Comparison of the direct colorimetry method with RAPIDEC CARBA NP for selected strains

496	<b>Strain</b>	<b><math>\beta</math>-lactamases</b>	<b>Direct colorimetry result</b>	<b>CARBA NP result/color</b>
497	<i>K. pneumoniae</i> LA30	VIM-1	Positive	Positive/Yellow
498	<i>E. coli</i> TZ116	VIM-1, CMY-13	Positive	Positive/Yellow
499	<i>P. mirabilis</i> EUG91	VIM-1, VEB-1	Positive	Positive/Yellow
500	<i>K. pneumoniae</i> 2489	NDM-1/CTX-M	Positive	Positive/Yellow
501	<i>K. pneumoniae</i> LA28	NDM-1/CTX-M	Positive	Positive/Yellow
502	<i>K. aerogenes</i> 7362	NDM-1	Positive	Positive/Yellow
503	<i>K. pneumoniae</i> E971	KPC-2, SHV-5 type	Positive	Positive/Yellow
504	<i>K. pneumoniae</i> E1370	KPC-2	Positive	Positive/Yellow
505	<i>E. coli</i> LAR548	KPC-2	Positive	Positive/Yellow
506	<i>K. pneumoniae</i> ALX47	OXA-48, CTX-M-15	Positive	Positive/Orange
507	<i>K. pneumoniae</i> LAR478	OXA-48, CTX-M-15	Positive	Positive/Orange
508	<i>K. pneumoniae</i> TRK1	OXA-48, CTX-M-15	Negative	Negative/Red
509	<i>K. pneumoniae</i> TRK-5	OXA-48, CTX-M-15	Positive	Negative/Red
510	<i>K. pneumoniae</i> EY-205	CMY-36/SHV-5	Negative	Positive/Orange
511	<i>K. pneumoniae</i> 17829	CTX-M-15/SHV-12	Negative	Positive/Orange
512	<i>K. aerogenes</i> EY-25	LAT-2/SHV-5	Negative	Negative/Red
513	<i>E. cloacae</i> EY 138	Derepressed AmpC	Negative	Negative/Red
514	<i>E. coli</i> IK33	CTX-M-15	Negative	Negative/Red

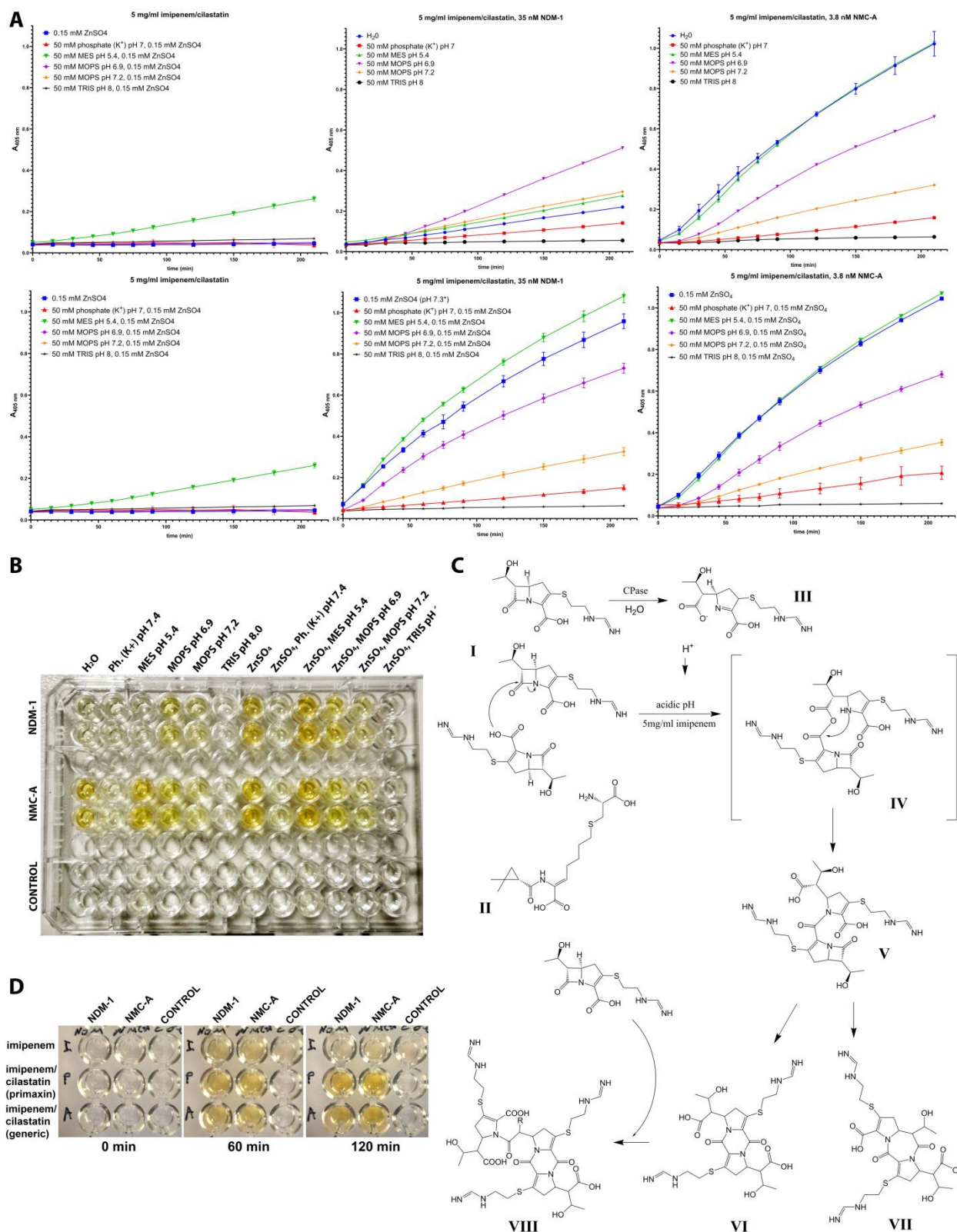
515  
516  
517  
518  
519  
520  
521  
522  
523  
524  
525  
526  
527  
528  
529  
530  
531  
532  
533  
534  
535  
536  
537  
538  
539  
540

541 **Figures**



554 **Figure 1: A)** Differential absorption spectra in the visible spectrum during incubation of various  $\beta$ -  
555 lactamases with 5 mg/ml imipenem/cilastatin. The efficient carbapenemases NDM-1 and NMC-A induced  
556 sharp absorbance shifts followed by the less potent OXA-48. Enzymes not exhibiting imipinemase activity  
557 caused marginal absorbance changes that were comparable to that of the control reaction. **B)** Absorbance  
558 increases in three wavelengths corresponding to the detected peaks in differential absorption spectra.  
559 Monitoring the absorbance increase at 405 nm can clearly differentiate carbapenemases from non-  
560 carbapenemases.

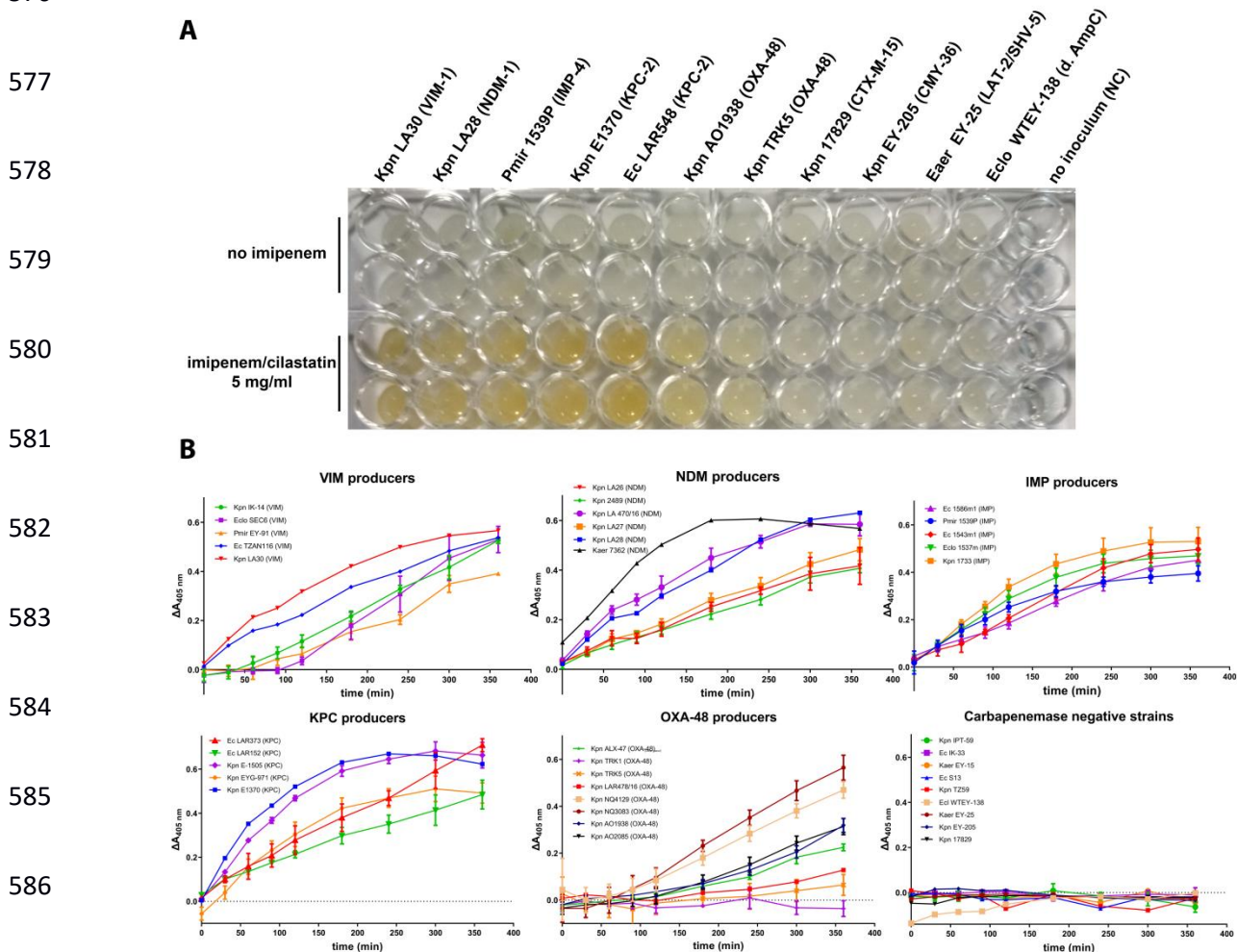
561



562 **Figure 2: A)** Effects of various buffers on the color development induced by NDM-1 and NMC-A in the  
 563 absence (upper panel) and presence (lower panel) of zinc cations estimated by absorbance measurements  
 564 at 405 nm. In NDM-1 containing reactions (medium column) color development is significantly enhanced



565 by zinc sulfate at a concentration of 0.15 mM while the class A carbapenemase NMC-A (right column)  
 566 yielded equivalent signals in both conditions. Color development was extended in acidic pH and in un-  
 567 buffered conditions, with high alkalinity attenuating the reaction. In control reactions lacking a  
 568 carbapenemase (left column) an absorbance increase was observed in the presence of 50 mM MES buffer  
 569 pH 5.4. **B)** Color development in the above conditions as documented at the final point (t=240 min). **C)** A  
 570 likely molecular mechanism for the carbapenemase induced yellow color. **CPase:** carbapenemase, **I:**  
 571 imipenem, **II:** cilastatin, **III:** hydrolyzed imipenem. Compounds **VI** and **VIII**, containing a diketopiperazine  
 572 ring, exhibit a  $\lambda_{max}$  at 360 nm and form yellow colored solutions (11). **D)** Effect of NDM-1 and NMC-A on  
 573 pure imipenem and on the brand name imipenem/cilastatin formulation (Primaxin) in comparison with  
 574 the generic imipenem/cilastatin formulation used in the study under the same conditions.  
 575 Imipenem/cilastatin reactions yielded stronger and more stable yellow color compared to pure imipenem.  
 576



587 **Figure 3:** Application of the imipenem decomposition method on bacterial suspensions. **A)** Color  
 588 development at the end point (t = 360 min) of enterobacterial strains' cell suspensions producing various  
 589 types of carbapenemases and  $\beta$ -lactamases with no imipenemase activity. **B)** Absorbance changes at 405  
 590 nm during the course of six hours in imipenem/cilastatin-bacterial suspensions mixtures of the strains  
 591 assayed in the study. M $\beta$ L and KPC producing strains yielded strong signals that could be detected as early

592 as 30 minutes. *K. pneumoniae* producing the OXA-48 class D carbapenemase yielded weaker responses  
 593 with one strain being identified as negative. The nine non-carbapenemase producers did not cause any  
 594 color shift even after six hours of incubation.

595

596

597

598

599

600

601

602

603

604

605

606

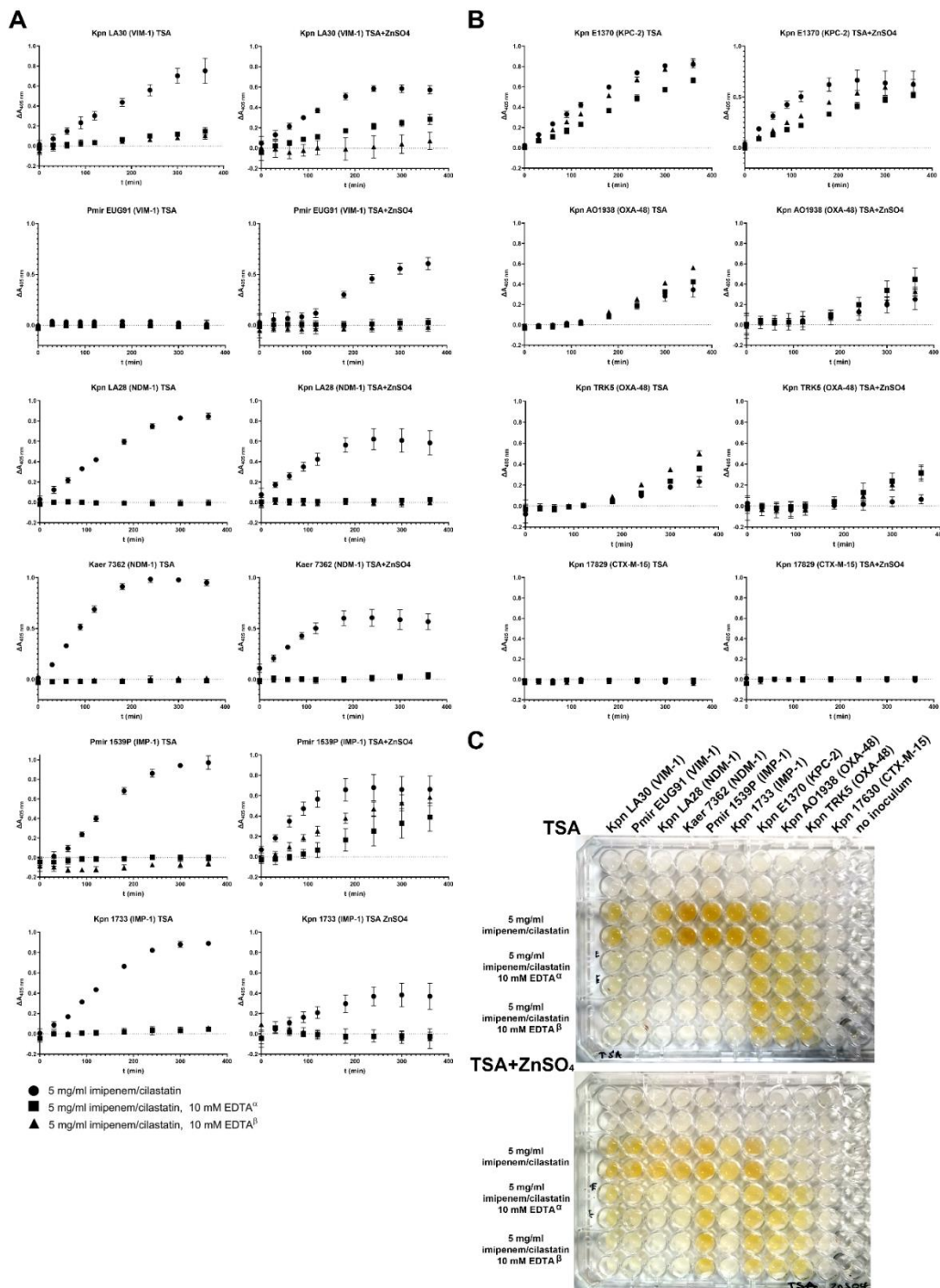
607

608

609

610

611 **Figure 4:** Differentiation of M $\beta$ L and class A carbapenemase producers through the use of EDTA and  
 612 effects of zinc cation supplementation of the growth medium. **(A)** Time courses of absorbance changes at  
 613 405 nm of M $\beta$ L producing strains in the presence and absence of 10 mM EDTA when bacteria were



614 cultured without (left panel) and with zinc supplementation (right panel) in the TSA medium. Experiments  
615 were performed with EDTA added in the wells prior to reactants' addition (black squares,  $\alpha$ ) or with  
616 bacterial cells suspended in a 20 mM EDTA solution (black triangles,  $\beta$ ). EDTA inhibited the decomposition  
617 of imipenem in the majority of M $\beta$ L strains when they were cultivated in the absence of zinc. *P. mirabilis*  
618 EUG91 did not yield any signal when grown on plain TSA. **(B)** Effects of EDTA and growth on zinc  
619 supplemented TSA on reactions containing strains producing serine reactive  $\beta$ -lactamases. **(C)** Coloration  
620 observed in the above experiments after six hours of incubation.

621

622

623

624